

CoSDA: Continual Source-Free Domain Adaptation

Haozhe Feng^{*1}, Zhaorui Yang^{*1}, Hesun Chen^{*1},
Tianyu Pang², Chao Du², Minfeng Zhu¹, Wei Chen¹, Shuicheng Yan²

¹State Key Lab of CAD&CG, Zhejiang University

²Sea AI Lab

Abstract

Without access to the source data, source-free domain adaptation (SFDA) transfers knowledge from a source-domain trained model to target domains. Recently, SFDA has gained popularity due to the need to protect the data privacy of the source domain, but it suffers from catastrophic forgetting on the source domain due to the lack of data. To systematically investigate the mechanism of catastrophic forgetting, we first reimplement previous SFDA approaches within a unified framework and evaluate them on four benchmarks. We observe that there is a trade-off between adaptation gain and forgetting loss, which motivates us to design a consistency regularization to mitigate forgetting. In particular, we propose a continual source-free domain adaptation approach named CoSDA, which employs a dual-speed optimized teacher-student model pair and is equipped with consistency learning capability. Our experiments demonstrate that CoSDA outperforms state-of-the-art approaches in continuous adaptation. Notably, our CoSDA can also be integrated with other SFDA methods to alleviate forgetting.

1. Introduction

Domain adaptation (DA) [3] aims to transfer features from a fully-labeled source domain to multiple unlabeled target domains. Prevailing DA methods perform the knowledge transfer by consolidating data from various domains and minimizing the domain distance [13, 20, 32, 44]. However, due to the privacy policy, we cannot access source domain data in most cases, where all data and computations must remain local and only the trained model is available [2, 38].

Source-free domain adaptation (SFDA) [24, 26, 29, 31] maintains the confidentiality of the domain data by transferring knowledge straight from a source-domain-trained model

^{*}Equal contribution. Work done during an internship at Sea AI Lab, Singapore. Correspondence to: Tianyu Pang <tianyupang@sea.com>, Wei Chen <chenweis@zju.edu.cn>.

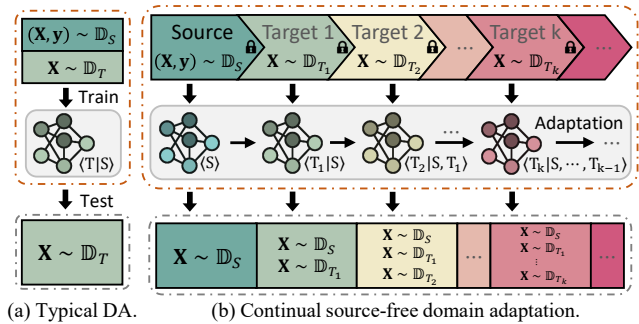


Figure 1. The illustration of continual DA. In typical DA (left), models are trained on both source and target domain but are only tested on target domain. In our CoSDA settings (right), the model is sequentially trained on each target domain and tested on all previously seen domains. At each step, the model can only use data from the current target domain and has no access to other domains.

to target domains. SFDA also allows for spatio-temporal separation of the adaptation process since the model-training on source domain is independent of the knowledge transfer on target domain. However, due to the lack of alignment with prior domain features, typical SFDA methods tend to overfit the current domain, resulting in catastrophic forgetting on the previous domains [5, 47, 50, 53]. This forgetting can lead to severe reliability and security issues in many practical scenarios such as autonomous driving [45] and robotics applications [25]. To address this issue, a possible solution is to preserve a distinct model for each domain, but this solution is impractical since (1) the model pool expands with the addition of new domains, and (2) obtaining the specific domain ID for each test sample is hard.

In this paper, we introduce a practical DA task named continual source-free domain adaptation (continual SFDA), with the primary goal of maintaining the model performance on all domains encountered during adaptation. The settings of continual SFDA are presented in Figure 1. We initiate the adaptation process by training a model in the fully-labeled

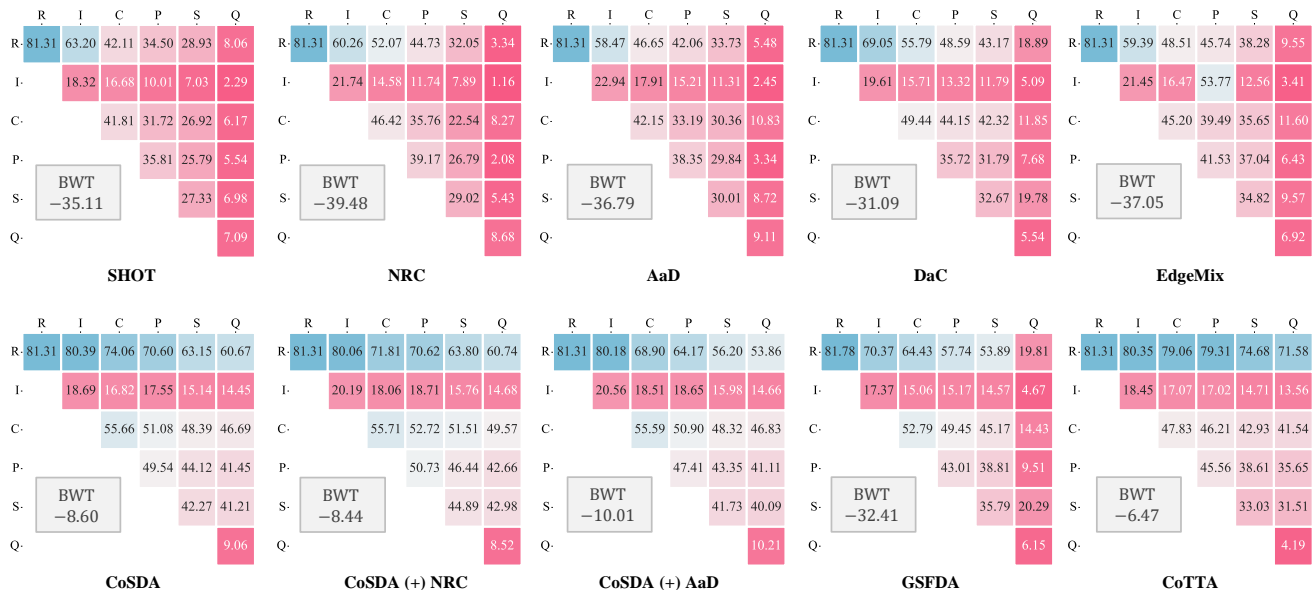


Figure 2. Multi-target sequential adaptation on the DomainNet with the adaptation order of **Real**→ **Infograph**→ **Clipart**→ **Painting**→ **Sketch**→ **Quickdraw**. The accuracy matrix is used to measure the transferability of the features. The value in position (i, j) denotes the accuracy on the i -th domain after adaptation on the j -th domain. Backward transfer (BWT) measures the total degree of forgetting with range -100 to 0 , where a larger BWT value indicates a smaller degree of forgetting and 0 indicates no forgetting.

source domain, and then subsequently transfer this off-the-shelf model in a sequential manner to each of the target domains. During the testing phase, data is randomly sampled from previously encountered domains, thereby rendering it impossible to determine the specific domain ID in advance.

To systematically investigate the mechanism of catastrophic forgetting, we reimplement previous SFDA approaches within a unified framework and conduct a realistic evaluation of these methods under the continual SFDA settings on four multi-domain adaptation benchmarks, i.e. DomainNet [40], Office31 [43], OfficeHome [49] and VisDA [41]. To ensure the representativeness of our evaluation, we select six commonly used SFDA methods as follows: SHOT [29], SHOT++ [31], NRC [52], AaD [54], DaC [58] and EdgeMix [23]. For further comparison, we also consider two well-performed continual DA methods: GSFDA [53] and CoTTA [50]. We measure the extent of forgetting exhibited by the aforementioned methods in both single-target and multi-target sequential adaptation scenarios. As shown in Figure 2, our experiments reveal two main findings: (1) the accuracy gain in the target domain often comes at the cost of huge forgetting in the source domain, especially for hard domains like quickdraw; (2) the catastrophic forgetting can be alleviated with data augmentations (e.g., DaC and Edgemix) and domain information preservation (e.g., GSFDA and CoTTA). Our investigation also finds some limitations of current continual DA techniques, such as GSFDA, which relies on domain ID information for each sample during testing, and CoTTA, which has a tendency

to overfit the source domain and learn less plastic features, leading to suboptimal adaptation performance.

In light of the above findings, we introduce CoSDA, a new **Continual Source-free Domain Adaptation** approach that reduces forgetting on all encountered domains and keeps adaptation performance on new domains through teacher-student consistency learning. CoSDA employs a dual-speed optimized teacher-student model pair: a slowly-changing teacher model to retain previous domain knowledge and a fast optimized student model to transfer to new domain. During adaptation, the teacher model infers on target domain to obtain knowledge that matches previous domain features, and the student model learns from this knowledge with consistency loss. We also incorporate mutual information loss to enhance the transferability and robustness to hard domains. Extensive experiments show that CoSDA significantly outperforms other SFDA methods in terms of forgetting index. Moreover, CoSDA does not require prior knowledge such as domain ID and is highly robust to hard domains. CoSDA is easy to implement and can be seamlessly integrated with other SFDA methods to alleviate forgetting.

2. Preliminaries and Related Works

Preliminaries. Let \mathbb{D}_S and \mathbb{D}_T denote the source domain and target domain. In domain adaptation, we have one fully-labeled source domain \mathbb{D}_S and K unlabeled target domains $\{\mathbb{D}_{T_k}\}_{k=1}^K$. To ensure confidentiality, all data computations are required to remain local and only the global model h is accessible, which is commonly referred to as source-free

domain adaptation [26, 29]. With this setting, continual DA starts from training an off-the-shelf model h on the source domain, and subsequently transfer it to all target domains. The goal of continual DA is to sustain the model’s performance on all previous domains after adaptation. We summarize two adaptation scenarios based on the number of target domains, as depicted in Figure 1:

Single target adaptation. We start from $K = 1$, which is most common for current SFDA studies. In this setting, A source pre-trained model is transferred to one target domain and test data is arbitrarily sampled from both source and target domain without prior knowledge such as domain ID.

Multi-target sequential adaptation. We extend to $K \geq 2$, where the model is sequentially transferred to each target domain and test data is drawn from all seen domains.

Related Works. Current SFDA methods adopt self-training techniques to address domain shift: SHOT [29] uses entropy regularization for adaptation; NRC [52] and AaD [54] generate pseudo-labels with nearest-neighbor; DaC [58] and EdgeMix [23] adopt data augmentation as consistency loss and SHOT++ [31] designs auxiliary tasks to learn domain-generalized features. Despite the above methods, we further survey two types of methods closely related to CoSDA: knowledge distillation-based methods and continual DA.

Knowledge distillation-based methods. Knowledge distillation [18], which transfers knowledge from a well-trained teacher model to a student model, has been widely used in domain adaptation. To enhance adaptation performance, bi-directional distillation is applied in TSML [27] while SSNLL [9] utilizes the mean-teacher [48] structure. DINE [30] introduces a memory-bank to store historical inference results, providing better pseudo-labels for the student model. However, in contrast to the dual-speed optimization strategy used in CoSDA, these distillation-based methods update both the teacher and student models simultaneously, leading to the forgetting of previous domain features.

Continual DA. A few works have explored continual domain adaptation by incorporating continual learning techniques, which can be summarized into three categories: feature replay [5], dynamic architecture [35, 36, 53] and parameter regularizations [39, 50]. CUA [5] samples a subset from each target domain as replay data. PackNet [35] separates a subset neurons for each task. Aadgraph [36] encodes the connection of previous domains into one dynamic graph and uses it to select features for new domain. GSFDA [53] assigns specific feature masks to different domains. EATA [39] uses the elastic-weight consolidation (EWC) [22] as the regularization loss. CoTTA [50] ensures knowledge preservation by stochastically preserving a subset of the source model’s parameters during each update. Distinct from the above methods, CoSDA adopts a dual-speed optimized teacher-student model pair, inspired by LSTM [19], to mitigate forgetting. Specifically, a slowly-changing teacher model is uti-

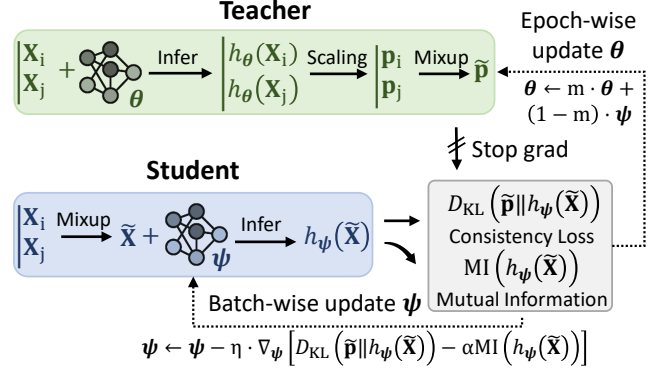


Figure 3. The pipeline of CoSDA. We use a dual-speed optimized teacher-student model pair to adapt to new domains while avoiding forgetting. The student model uses teacher knowledge as pseudo-labels and creates consistency loss with mixup. Mutual information is employed to improve the robustness on hard domain. During training, the student model is updated with SGD after each batch, while the teacher model is updated with EMA after each epoch.

lized to preserve long-term features, while a fast optimized student model is employed to learn domain-specific features.

3. CoSDA: An Approach for Continual SFDA

Overview. CoSDA is a continual source-free domain adaptation method that achieves multi-target sequential adaptation through pseudo-label learning. For continual learning, CoSDA uses the features learned from previous domains to construct pseudo-labels, which are then used for both adapting to new target domains and preventing forgetting on previously encountered domains. Inspired by knowledge distillation [18, 59], CoSDA utilizes a dual-speed optimized teacher-student model pair, consisting of the teacher model h_θ which retains the knowledge of previous domains, and the student model h_ψ that learns domain-specific features. The teacher model generates pseudo-labels for the student model during training, and the student model learns from both the target data and the pseudo-labels using a consistency loss. After adaptation, the teacher model serves as the global model. The framework of CoSDA is presented in Figure 3, and the details are discussed below.

3.1. Consistency Learning with Teacher Knowledge

For each data point \mathbf{X} from current target domain \mathbb{D}_{T_k} , we obtain the classification score from the teacher model $h_\theta(\mathbf{X})$, and use it as the pseudo-label to train the student model. However, directly learning from $h_\theta(\mathbf{X})$ may lead to overfitting to the teacher model. To address this issue, we introduce a consistency loss that consists of three steps. First, we compress the soft-label $h_\theta(\mathbf{X})$ into a hard-label \mathbf{p} with a temperature parameter τ as $\mathbf{p} := \text{softmax}(h_\theta(\mathbf{X})/\tau)$. Next, we augment \mathbf{X} and train the student model to consist with the hard-label \mathbf{p} for the augmented samples. Among existing

methods [8, 10, 34]. We choose mixup [55] as the augmentation strategy for three advantages: (1) Mixup has the lowest computation cost. Non-mixup augmentation methods typically require $k \times$ data-augmentations and model inferences for each sample (e.g., $k = 4$ for MixMatch [4] and 32 for CoTTA [50]), while mixup works with $k = 1$ and therefore does not require any extra computations. (2) Mixup can be applied to other data modalities, such as NLP [15] and Audio [37], while other methods are specifically designed for image data. (3) Mixup facilitates the learning of domain-invariant features. Recent studies [6, 56] point out that mixup can contract the data points towards their domain centroid, thereby holistically reducing the domain distance (details are provided in Appendix A.1). With mixup augmentation, we construct the consistency loss as follows:

Consistency learning with mixup. For a random-sampled data pair $(\mathbf{X}_i, \mathbf{X}_j)$ with hard-labels $(\mathbf{p}_i, \mathbf{p}_j)$. We sample $\lambda \sim \text{Beta}(a, a)$ and construct the mixed data point as

$$\tilde{\mathbf{X}} = \lambda \mathbf{X}_i + (1 - \lambda) \mathbf{X}_j; \quad \tilde{\mathbf{p}} = \lambda \mathbf{p}_i + (1 - \lambda) \mathbf{p}_j, \quad (1)$$

then the consistency loss for h_ψ is

$$\ell_{\text{cons}}(\tilde{\mathbf{X}}, \tilde{\mathbf{p}}; \psi) := D_{\text{KL}}(\tilde{\mathbf{p}} \| h_\psi(\tilde{\mathbf{X}})). \quad (2)$$

Consistency loss helps student model to learn from both previous domain knowledge and the target domain features. However, when the target data is extremely different from the previous domains, the consistency loss may cause the model collapse. To improve the robustness of the model and enable it to learn from hard domains, we employ the mutual information (MI) loss as the regularization:

Mutual information maximization. For a batch of mixed data $\{\tilde{\mathbf{X}}_i\}_{i=1}^B$, we obtain the marginal inference results as $\bar{\mathbf{h}}_\psi = \frac{1}{B} \sum_{i=1}^B h_\psi(\tilde{\mathbf{X}}_i)$ and formalize the MI as follows:

$$\text{MI}(\{h_\psi(\tilde{\mathbf{X}}_i)\}_{i=1}^B) := -\frac{1}{B} \sum_{i=1}^B D_{\text{KL}}(h_\psi(\tilde{\mathbf{X}}_i) \| \bar{\mathbf{h}}_\psi). \quad (3)$$

Our goal is to maximize mutual information during training, which is achieved through the related MI loss as $\ell_{\text{MI}} := -\text{MI}(\cdot)$. Based on previous studies [21, 29], ℓ_{MI} can be decomposed into two components: maximizing the instance entropy and minimizing the marginal inference entropy. The former encourages the model to learn distinct semantics for each data sample, while the latter prevents the model from overfitting to only a few classes (see Appendix A.2 for detailed analysis). Experimental results demonstrate that using the MI loss enables CoSDA to adapt to hard domains (such as Quickdraw on DomainNet) without experiencing catastrophic forgetting. The total loss is obtained by combining the consistency loss and MI loss, i.e., $\ell_\psi = \ell_{\text{cons}} + \alpha \cdot \ell_{\text{MI}}$.

3.2. Dual-Speed Optimization Strategy

In continual domain adaptation, the global model adapts to each target domain in sequence. To prevent forgetting of previously learned features, we are inspired by LSTM for sequence data processing and adopt a dual-speed strategy to optimize the student and teacher models separately, with the student learning short-term features specific to the current domain and the teacher filtering out long-term domain-invariant features. Specifically, the student model is updated rapidly using SGD with loss ℓ_ψ after every batch, while the teacher model is slowly updated by performing exponential moving average (EMA) between the previous-step teacher model and the current-step student model at the end of each epoch, as depicted in Figure 3. This dual-speed strategy allows for a smooth knowledge transition between the two models, preventing abrupt changes during adaptation and maintaining the model’s performance on previous domains.

Updating the mean and variance in BatchNorm. BatchNorm is a widely-used normalization technique in deep learning models, which estimates the mean and variance of the overall dataset as $(\boldsymbol{\mu}, \mathbf{Var})$ and utilizes these statistics to normalize the data. As the $\boldsymbol{\mu}$ - \mathbf{Var} statistics can exhibit significant variation across different domains, prior DA methods, such as FedBN [28] and DSBN [7], typically assign distinct statistics to different domains. However, these methods are not applicable to continual DA since the test data randomly comes from all previously encountered domains without prior knowledge of the domain ID. To unify the BN statistics among different domains, we propose a dual-speed updating method for the mean and variance values. During the training process, the student model estimates the mean and variance of the target domain data as $\boldsymbol{\mu}_\psi$ and \mathbf{Var}_ψ respectively. After each epoch, the teacher model updates its BN statistics using the EMA method illustrated above as:

$$\boldsymbol{\mu} \leftarrow m\boldsymbol{\mu} + (1 - m)\boldsymbol{\mu}_\psi; \quad \mathbf{Var} \leftarrow m\mathbf{Var} + (1 - m)\mathbf{Var}_\psi. \quad (4)$$

During testing, the teacher model applies the global $(\boldsymbol{\mu}, \mathbf{Var})$ parameters to BatchNorm without the need for domain ID.

3.3. Algorithm and Hyper-parameters

Based on the concepts of consistency learning and dual-speed optimization, we present the operating flow of our CoSDA method in Algorithm 1 as follows: at first, we initialize the teacher and student models with the global model that has been trained on previous domains. During each epoch, we employ consistency learning to train the student model while keeping the teacher model frozen. When an epoch is finished, we use EMA to update the teacher model as well as the mean and variance statistics of BatchNorm. After adaptation, the teacher model serves as the new global model.

CoSDA is easy to *integrate with other SFDA methods* to further mitigate the forgetting. As outlined in Section 3.1,

Algorithm 1 Adaptation process of CoSDA for \mathbb{D}_{T_k}

- 1: **Inputs:** global model h , unlabeled training set \mathbb{D}_{T_k} .
 - 2: **Hypars:** total epochs E , learning rate η , temperature τ , mixup Beta(a, a), loss weight α , EMA momentum m .
 - 3: Initialize $\theta \leftarrow h, \psi \leftarrow h, (\mu, \mathbf{Var}) \leftarrow h$;
 - 4: **for** $t = 0$ **to** $E - 1$ **do**
 - 5: **for** every mini-batch \mathbf{X} **in** \mathbb{D}_{T_k} **do**
 - 6: Init. $\mathbf{p} = \text{softmax}(h_\theta(\mathbf{X})/\tau), \lambda \sim \text{Beta}(a, a)$;
 - 7: Mixup. $(\tilde{\mathbf{X}}, \tilde{\mathbf{p}}) = \lambda(\mathbf{X}, \mathbf{p}) + (1 - \lambda)\text{Shuffle}(\mathbf{X}, \mathbf{p})$;
 - 8: Infer. $\ell(\tilde{\mathbf{X}}, \tilde{\mathbf{p}}; \psi) = \ell_{\text{cons}}(\tilde{\mathbf{X}}, \tilde{\mathbf{p}}; \psi) + \alpha \ell_{\text{MI}}(\tilde{\mathbf{X}}; \psi)$;
 - 9: SGD. $\psi \leftarrow \psi - \eta \cdot \nabla_\psi \ell(\tilde{\mathbf{X}}, \tilde{\mathbf{p}}; \psi)$; # *Student*
 - 10: **end for**
 - 11: EMA. $\theta \leftarrow m \cdot \theta + (1 - m) \cdot \psi$; # *Teacher*
 - 12: EMA. $\mu \leftarrow m \cdot \mu + (1 - m) \cdot \mu_\psi$;
 - 13: EMA. $\mathbf{Var} \leftarrow m \cdot \mathbf{Var} + (1 - m) \cdot \mathbf{Var}_\psi$.
 - 14: **end for**
 - 15: **Return:** new global model h with params $(\theta, \mu, \mathbf{Var})$.
-

the pseudo-labels for the student model are simply generated by compressing the soft-label from the teacher model. The quality of these pseudo-labels can be further enhanced with advanced SFDA methods such as the memory bank [52, 30], kNN [54], and graph clustering [51]. By further refining the inference results from the teacher model, these pseudo-label-based methods can be seamlessly integrated with CoSDA. The results on both single target (Figure 2,4) and multi-target sequential adaptation (Table 1,2, and 3) extensively show that the integration of CoSDA significantly reduces forgetting while maintaining adaptation performance.

Implementation details of CoSDA. We introduce four hyper-parameters: label compression temperature (τ), mixup distribution (a), loss weight (α) and EMA momentum (m). Following prior research on knowledge distillation [18] and mixup [4], we fix $\tau = 0.07$ and $a = 2$ for all experiments. Our findings suggest that the mutual information (MI) loss function performs well on datasets with a small number of well-defined classes and clear class boundaries, but it may lead to incorrect classification on datasets with a large number of classes exhibiting semantic similarity. Therefore, we set α empirically to 1 for OfficeHome, Office31 and VisDA, and 0.1 for DomainNet. To apply the EMA strategy, we follow the settings in MoCo [17] and BYOL [14] and increase the momentum from 0.9 to 0.99 using a cosine schedule as

$$m_t = 0.99 - 0.1 \times \left[\cos\left(\frac{t}{E}\pi\right) + 1 \right] / 2.$$

4. Experiments

We investigate the mechanisms of catastrophic forgetting through a systematic analysis of various continual DA scenarios. First, we conduct extensive experiments on representative methods from SFDA and continual DA, and

report their forgetting on several benchmarks. Then we demonstrate the effectiveness of CoSDA in reducing forgetting under both single and multi-target sequential adaptation scenarios. We also analyze the robustness of CoSDA to hard domains. To ensure fairness in comparison, we reimplement the selected methods in a unified framework. **The code** used to reproduce our results is provided in [Github](#).

4.1. Realistic Evaluation of Current Methods

To avoid unfair comparisons that can arise from variations in the backbones, pretraining strategies, total training epochs, and benchmark datasets, we implemented several representative SFDA methods in a unified framework and evaluated them on four benchmarks: DomainNet [40], OfficeHome [49], Office31 [43], and VisDA [41]. In detail, we employ the ImageNet-pretrained ResNet with a weight-normed feature bottleneck [31] as the backbone, utilize the dual-lr pre-training strategy proposed in SHOT [29], and adopt mini-batch SGD with momentum 0.9 as the optimizer. The total number of epochs is set to 20 and batch size is 64. For model-specific hyperparameters, please refer to Appendix B.

Without loss of generality, we selected six representative methods: (1) SHOT [29] and SHOT++ [31] as they are the first to propose the SFDA setting and have been followed by many works such as DINE [30], CPGA [42], and Decision [1]. (2) NRC [52] and AaD [54] as they perform the best on all benchmarks and can integrate with CoSDA. (3) DaC [58] and Edgemix [23] as they both use data augmentations to construct consistency loss for adaptation, which is similar to our approach. For comparison, we consider two well-performed continual DA methods: GSFDA [53] and CoTTA [50]. We report the adaptation performance and forgetting loss of the above methods on both single-target and multi-target sequential adaptation settings:

For single target adaptation, we traverse all domain combinations and report both the adaptation accuracy on the target domain and the accuracy drop on the source domain.

For multi-target adaptation, we follow the studies on the domain distances [40, 57] and select the shortest path for sequential adaptation, i.e., **Real** \rightarrow **Infograph** \rightarrow **Clipart** \rightarrow **Painting** \rightarrow **Sketch** \rightarrow **Quickdraw** for DomainNet and **Art** \rightarrow **Clipart** \rightarrow **Product** \rightarrow **Real-world** for OfficeHome. Following the continual learning protocols [33, 16], we construct an accuracy matrix $\mathbf{R} \in \mathbb{R}^{K \times K}$ over K target domains, where $\mathbf{R}_{i,j}$ is the accuracy on the i -th domain after adaptation on the j -th domain. The accuracy matrix \mathbf{R} is reported to measure the transferability of the features. Moreover, we use backward transfer (BWT) to measure the degree of forgetting, which is calculated as $\text{BWT} = \frac{1}{K-1} \sum_{i=1}^{K-1} \mathbf{R}_{i,K} - \mathbf{R}_{i,i}$. BWT ranges from -100 to 0 , with -100 indicating the complete forgetting and 0 indicating no forgetting.

Table 1. Single target adaptation on DomainNet with six domains denoted as **R** (real), **I** (infograph), **C** (clipart), **P** (painting), **S** (sketch) and **Q** (quickdraw). **Vanilla** refers to the accuracy of applying the source-trained model directly to the target domain without adaptation. **(-)** **MI** refers to removing the mutual information loss from CoSDA, **(+)** **NRC** and **(+)** **AaD** refers to integrating CoSDA with NRC and AaD. Results are reported as: **Adaptation accuracy (%) on the target domain | Accuracy drop (%) on the source domain**.

DA	Vanilla	SHOT	SHOT++	NRC	AaD	DaC	EdgeMix	GSFDA	CoTTA	CoSDA	CoSDA (-) MI	CoSDA (+) NRC	CoSDA (+) AaD
I2R	44.99	59.89 13.69	60.14 15.95	59.64 14.44	60.19 14.18	54.86 9.21	60.07 12.87	52.12 7.50	48.00 0.64	55.75 3.27	55.64 4.95	59.19 4.34	58.21 2.73
C2R	50.83	62.80 18.03	62.47 17.51	64.14 20.40	63.20 23.33	58.83 13.47	64.70 19.06	55.26 2.59	53.60 0.87	60.31 4.16	59.92 6.14	61.29 4.13	61.04 3.66
P2R	57.20	62.94 14.76	62.62 13.68	64.50 14.22	64.15 17.94	60.97 6.91	65.36 15.67	58.18 2.78	58.24 0.26	61.56 1.22	61.37 3.46	63.21 3.37	62.84 3.21
S2R	45.41	61.84 21.43	62.32 19.03	62.83 15.66	62.29 25.61	59.26 19.95	63.64 22.00	56.25 6.12	51.56 0.33	60.62 4.42	60.22 7.02	60.32 5.54	60.11 4.38
Q2R	5.17	33.55 55.87	34.62 58.96	35.59 60.46	38.74 62.29	25.76 34.91	35.19 55.61	20.53 25.29	14.09 14.13	19.93 19.54	—	24.58 20.69	24.99 16.44
Avg.	40.72	56.20 24.76	56.43 25.03	57.34 25.04	57.71 28.67	51.94 14.89	57.79 25.04	48.47 8.86	45.10 3.25	51.63 6.52	—	53.72 7.61	53.44 6.08
R2I	17.36	18.30 18.11	18.72 18.46	21.74 21.05	23.06 22.91	19.61 12.32	21.45 21.92	17.37 11.41	18.41 2.60	18.68 0.38	19.77 12.22	20.18 11.25	20.55 11.13
C2I	14.59	15.51 22.47	15.97 21.71	17.88 31.70	19.92 24.24	15.31 23.78	17.94 26.29	14.21 18.99	15.87 2.08	16.73 3.74	—	20.78 6.24	20.44 7.29
P2I	15.23	16.86 17.21	16.64 18.06	18.28 21.60	19.65 20.31	17.18 15.17	18.46 22.25	15.84 12.47	16.33 2.50	17.76 2.82	17.87 2.01	20.27 5.73	20.65 8.51
S2I	11.86	16.72 20.81	16.53 23.77	18.89 16.14	20.04 17.29	16.69 18.12	18.43 20.43	14.66 13.66	14.70 3.05	12.94 2.62	15.18 3.06	20.22 19.39	20.33 9.60
Q2I	1.09	3.38 46.04	4.47 55.57	5.98 43.99	6.96 48.47	4.03 49.38	7.18 56.35	3.03 50.07	2.54 19.73	2.05 4.24	—	5.66 13.34	5.43 10.27
Avg.	12.03	14.15 24.93	14.47 27.51	16.55 26.90	17.93 26.64	14.56 23.75	16.69 29.45	13.02 19.32	13.57 5.99	13.63 2.76	—	17.42 17.19	17.48 17.36
R2C	45.62	54.82 21.71	56.09 21.17	56.42 20.64	57.54 26.62	52.12 12.52	57.66 21.23	49.53 6.97	48.26 1.13	56.37 6.29	55.83 6.11	56.64 6.92	56.85 7.98
I2C	30.46	45.67 14.82	46.32 14.80	44.13 18.01	47.12 13.43	39.35 10.40	46.06 13.79	32.81 18.00	33.12 1.14	41.57 6.02	40.97 8.07	45.65 6.68	46.42 7.13
P2C	40.74	50.84 23.33	50.77 22.41	51.82 22.39	53.40 22.91	45.61 14.48	52.87 21.50	44.19 19.61	43.92 2.23	50.88 7.66	50.49 6.53	52.73 7.53	52.05 7.62
S2C	47.48	57.26 15.98	58.19 14.72	58.93 14.16	60.28 15.51	55.79 9.48	59.35 12.66	54.06 5.73	52.00 0.09	61.28 5.49	60.60 5.32	59.24 5.44	60.22 6.10
Q2C	10.33	33.61 34.80	35.92 38.95	38.44 44.27	39.19 43.13	31.54 39.68	38.61 43.81	26.94 20.68	23.20 8.98	32.96 14.58	32.88 26.88	34.13 14.39	34.55 15.07
Avg.	34.89	48.45 22.13	49.46 22.41	49.95 23.89	51.51 24.32	44.88 15.57	50.91 22.60	41.51 10.20	40.10 2.71	48.61 8.01	48.15 10.58	49.68 8.19	50.02 8.78
R2P	45.54	50.74 17.73	50.65 17.77	52.94 14.06	53.34 19.85	50.94 15.46	53.05 12.68	49.22 13.71	47.50 0.35	54.29 4.47	53.78 5.03	54.44 4.67	53.96 6.71
I2P	29.09	41.57 12.34	42.38 14.75	41.80 12.99	44.47 13.42	39.61 17.15	43.18 13.90	35.71 5.72	32.40 0.74	42.40 4.61	42.52 5.30	44.69 4.86	44.27 4.76
C2P	33.13	42.92 18.16	43.64 16.26	44.72 18.65	45.09 19.68	41.32 14.49	44.68 16.30	37.92 13.59	36.44 1.17	44.12 4.42	44.39 6.19	45.27 4.66	45.52 6.60
S2P	32.81	46.51 14.13	46.91 13.27	48.59 12.78	48.59 12.78	47.04 9.14	47.85 13.68	43.96 5.95	40.13 0.42	50.62 4.85	49.90 5.44	48.52 6.04	48.32 6.56
Q2P	1.79	15.27 47.94	18.55 51.85	18.87 62.80	23.52 63.75	14.48 37.73	21.04 63.47	10.03 31.70	6.53 16.29	9.47 14.32	—	14.81 13.47	16.70 14.20
Avg.	28.47	39.40 20.06	40.43 20.40	41.29 24.35	43.00 25.90	38.68 14.79	41.96 24.01	35.37 10.13	32.60 3.79	40.18 6.53	—	41.55 6.74	41.75 7.77
R2S	32.42	40.04 24.19	40.96 23.46	44.19 22.56	43.87 13.27	40.52 18.97	44.37 24.03	41.70 14.03	36.44 2.17	43.35 8.81	43.77 8.60	46.07 8.18	45.15 10.00
I2S	24.44	32.45 18.99	35.17 19.37	34.37 17.27	37.73 16.77	30.04 14.04	35.19 17.31	27.52 16.41	27.40 1.78	32.32 6.05	32.53 11.17	36.61 5.56	37.07 6.11
C2S	38.40	43.86 16.25	44.59 12.95	46.25 14.30	47.14 15.94	41.41 13.10	45.98 18.61	41.70 17.53	40.53 1.39	46.11 4.05	46.43 4.93	47.67 3.95	47.21 5.72
P2S	33.89	40.07 21.53	41.14 19.95	43.64 16.17	43.39 23.70	41.05 12.77	42.93 19.71	39.04 15.41	37.45 3.25	43.29 6.01	43.81 6.77	44.86 5.61	44.38 8.13
Q2S	8.23	23.43 35.69	24.49 35.29	29.54 47.71	27.65 48.55	22.20 27.02	30.31 45.97	14.58 43.90	13.68 7.20	17.14 10.06	—	23.48 13.77	24.34 14.81
Avg.	27.48	35.97 23.33	37.27 22.20	39.60 23.60	39.96 27.25	35.04 17.18	39.76 25.21	32.91 19.46	31.10 3.16	36.44 7.00	—	39.74 7.41	39.63 8.95
R2Q	4.54	7.08 69.33	8.32 70.96	8.14 72.13	10.81 66.83	8.73 55.82	7.62 73.35	6.15 61.61	6.40 7.49	6.01 2.95	—	7.04 5.34	8.58 5.71
I2Q	2.36	4.97 28.45	5.21 31.29	4.28 31.28	6.89 30.99	3.38 28.18	4.91 31.53	2.89 27.20	3.20 8.41	2.97 1.80	—	3.07 2.99	5.11 8.96
C2Q	9.56	14.31 57.27	14.07 62.85	15.19 62.36	18.23 52.51	12.02 50.44	14.47 64.73	11.86 65.98	11.57 6.11	11.58 2.07	8.50 7.97	12.72 2.20	15.89 8.24
P2Q	3.40	8.14 61.03	9.52 60.04	9.19 59.95	12.10 63.10	8.16 51.93	9.61 64.70	6.50 57.15	6.19 12.41	5.12 3.77	—	5.70 2.98	8.99 9.00
S2Q	11.11	14.55 49.63	14.65 45.13	15.37 37.25	18.59 42.09	14.32 36.74	15.32 38.15	14.73 34.21	12.62 4.59	12.66 2.61	10.56 8.66	16.34 10.57	17.61 6.84
Avg.	6.19	9.81 53.14	10.35 54.05	10.43 52.59	13.32 51.10	9.32 44.62	10.39 54.49	8.43 49.23	8.00 7.80	7.67 2.64	—	8.97 4.82	11.24 7.75

Table 2. Single target adaptation on OfficeNet (with A (art), C (clipart), P (product) and R (real-world)) and Office31 (with A (amazon), D (dslr) and W (webcam)). Results are reported as: **Adaptation accuracy (upper) and Accuracy drop (lower)**.

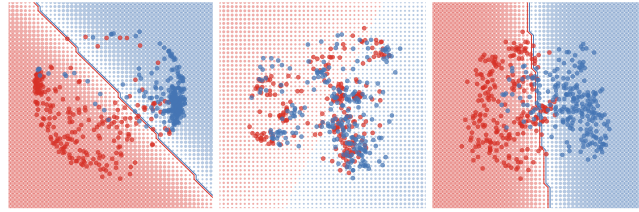
Method	OfficeHome													Office31							
	C2A	P2A	R2A	A2C	P2C	R2C	A2P	C2P	R2P	A2R	C2R	P2R	Avg.	D2A	W2A	A2D	W2D	A2W	D2W	Avg.	
Vanilla	48.98	67.09	74.57	50.68	63.14	64.15	50.89	42.27	73.26	63.82	48.66	77.90	60.45	78.11	71.82	94.34	98.59	57.29	61.06	76.87	
SHOT	66.96	65.10	72.89	58.01	57.34	60.25	75.60	76.21	82.95	79.50	76.11	81.39	71.03	73.30	74.12	88.76	100.00	89.81	97.99	87.33	
	17.66	9.85	6.84	17.00	11.49	12.32	11.54	16.38	6.61	7.96	15.48	7.62	11.73	8.23	6.79	6.14	0.13	7.10	0.20	4.77	
SHOT++	67.04	65.84	72.31	59.59	58.76	62.70	76.19	76.44	83.49	79.57	76.75	81.89	71.71	74.62	75.65	88.76	100.00	92.08	97.99	88.18	
	16.28	11.47	8.79	15.50	12.03	12.11	12.61	16.70	8.19	8.90	16.74	7.57	12.24	7.03	9.18	6.95	0.25	6.95	0.40	5.13	
NRC	66.05	64.81	72.19	60.16	58.28	61.56	77.61	75.76	83.40	80.15	76.61	78.56	71.26	75.68	74.72	93.57	100.00	92.70	98.24	89.15	
	22.58	20.37	20.17	16.65	23.66	25.29	12.53	22.29	10.69	14.26	19.08	15.43	18.58	11.24	8.18	9.55	0.00	8.73	0.20	6.32	
AaD	70.91	67.57	73.75	60.25	60.60	60.94	78.46	76.41	84.46	81.75	78.91	81.59	72.97	75.43	75.61	93.57	99.80	92.20	98.49	89.18	
	23.82	17.87	12.48	19.66	16.06	15.95	14.55	21.19	8.35	12.16	18.69	11.38	16.01	10.64	14.21	8.52	0.00	7.10	0.00	6.74	
DaC	66.71	65.22	72.31	58.76	57.18	61.35	74.82	74.75	82.16	80.19	76.25	80.56	70.86	73.91	75.36	89.75	100.00	90.57	98.49	88.01	
	12.64	7.55	6.86	11.95	8.13	9.34	8.90	9.87	4.84	4.49	9.16	4.03	8.15	5.42	3.65	4.40	0.00	4.08	0.00	2.93	
EdgeMix	66.50	63.95	71.24	58.03	54.73	60.92	77.25	74.41	83.28	79.73	75.05	79.41	70.37	75.04	72.42	91.57	99.80	91.07	98.36	88.04	
	12.25	11.02	4.45	5.61	5.97	10.51	9.15														

Table 3. Single target domain on VisDA with the source domain *Synthetic* and target domain *Real*. Results are reported on each of the 12 classes separately, and the ablation study of CoSDA is conducted by successively removing the teacher model, dual-speed optimization, mixup, and mutual information loss.

Method	Plane	Beyel	Bus	Car	Horse	Knife	Motor	Person	Plant	Shovel	Train	Truck	Avg.
Vanilla	62.84	16.59	58.6	64.59	66.31	3.71	80.33	29.56	65.78	24.17	89.86	12.41	47.9
SHOT	95.58	85.64	85.44	71.22	95.84	96.19	85.85	85.65	91.25	89.00	84.47	48.41	84.55
	1.33	0.68	51.45	31.88	2.84	1.33	52.48	0.58	0.46	20.21	19.75	3.33	15.53
NRC	95.56	87.54	82.11	63.11	95.01	93.44	88.52	80.43	95.25	88.46	87.69	62.18	84.94
	0.08	0.20	27.39	34.81	11.23	0.36	16.77	7.60	1.67	9.82	34.04	13.90	13.16
AaD	95.39	86.35	82.87	69.63	95.18	95.13	89.77	82.52	91.58	90.92	90.20	57.60	85.60
	1.30	1.17	59.10	13.58	11.51	9.84	26.62	8.28	0.71	10.53	21.97	33.29	16.49
DaC	95.78	81.93	83.69	80.20	96.83	97.06	94.10	81.40	94.77	94.21	90.82	45.28	86.34
	0.10	0.34	40.44	30.15	9.08	1.66	14.13	7.29	0.33	1.52	13.97	2.58	10.12
EdgeMix	95.07	88.05	84.72	70.89	95.48	93.44	83.16	78.14	92.37	89.30	88.40	48.47	83.96
	0.65	0.94	28.31	31.11	7.84	0.32	33.45	14.30	0.54	7.68	24.74	16.69	13.88
GSFDA	96.32	90.73	83.73	69.20	96.53	92.34	86.09	80.58	93.76	92.81	88.62	45.17	84.66
	0.07	2.04	-0.24	29.30	5.05	0.00	33.99	1.07	0.19	4.28	15.44	9.79	8.41
CoTTA	94.50	60.14	92.62	71.20	96.08	38.41	96.13	81.39	94.61	85.39	84.57	30.81	77.15
	0.42	0.38	2.72	29.78	10.49	2.16	14.59	6.51	0.05	-0.02	15.07	19.48	8.47
CoSDA	94.99	80.69	86.99	73.41	94.75	85.97	93.58	79.72	93.11	85.75	90.25	37.71	83.08
(+) NRC	0.24	0.18	24.44	17.19	2.18	4.24	9.08	2.59	0.08	1.26	6.68	14.86	6.92
CoSDA	95.29	83.29	82.46	68.65	95.33	90.69	91.66	80.80	93.45	85.05	89.91	54.27	84.24
(+) AaD	0.23	0.16	31.43	25.83	1.70	1.30	18.15	1.78	0.11	9.53	8.94	9.75	9.08
Ablation Study													
CoSDA	95.04	86.76	86.69	75.13	95.58	90.98	91.95	82.66	93.38	88.99	90.01	51.30	85.71
	0.19	0.65	27.59	34.61	3.11	1.55	17.91	11.50	0.46	5.40	14.30	12.84	10.84
(-) Teacher	89.22	77.61	73.89	28.45	64.97	34.19	79.11	58.75	73.76	71.35	66.94	60.32	64.88
	0.49	95.93	86.19	98.04	89.28	96.45	93.02	99.41	87.89	96.03	94.62	87.23	85.38
(-) Dual-Speed	94.55	84.72	86.09	63.01	94.11	94.84	89.04	81.53	92.19	90.18	86.64	53.44	84.19
	1.08	9.63	28.29	57.40	21.86	12.25	49.08	37.74	2.40	9.59	33.68	32.48	24.62
(-) Mixup & MI	93.36	55.94	85.52	74.07	94.33	61.40	95.20	80.25	92.72	75.00	86.75	34.62	77.43
	0.06	0.43	0.79	17.23	4.69	0.06	5.35	7.23	0.06	-0.04	10.79	12.13	4.89
(-) Mixup	94.26	78.10	85.05	71.23	94.78	84.58	91.97	82.17	92.58	87.02	85.86	42.03	82.47
	0.24	1.10	10.34	25.21	8.71	0.21	16.65	9.22	0.35	0.37	19.03	13.06	8.71
(-) MI	94.45	72.94	89.16	76.90	95.99	74.87	94.22	79.21	93.82	72.41	88.86	29.68	80.21
	0.10	1.07	25.14	39.05	3.63	0.06	17.44	8.12	0.40	0.38	6.66	8.04	9.17

also impairs the model’s ability to adapt to new domains. For single target adaptation, although NRC and AaD suffer from catastrophic forgetting, they still achieve the best performance on the target domain. However, in multi-domain settings, their performance on subsequent domains becomes much lower than CoSDA. By integrating CoSDA with other SFDA methods, we can simultaneously mitigate catastrophic forgetting and enhance the model’s transferability to new domains. For example, by integrating CoSDA with NRC, we improve the BWT from -39.48 to -8.44 on DomainNet, accompanied by an average increase of 12.34% adaptation accuracy on the *clipart*, *painting*, and *sketch*. Similarly, integrating CoSDA with AaD resulted in an increase in BWT from -36.79 to -10.01 on DomainNet, accompanied by an average improvement of 11.31% in adaptation accuracy.

Comparison among continual DA methods. In single domain adaptation (Sec 4.2), we discuss the limitations of GSFDA and CoTTA, with GSFDA relying on domain ID during testing and CoTTA having suffered from limited transferability. These limitations become more severe in multi-domain settings. For instance, GSFDA needs to store features for each domain, leading to a decrease in transferability and difficulty in fitting to hard domains in large-scale datasets with many categories, such as DomainNet. However, in benchmarks with a small number of categories such as OfficeHome, GSFDA performs well in both transferability and mitigating catastrophic forgetting. CoTTA tends to overfit to the source domain, leading to a continuous drop in performance on the target domain until it becomes unfeasible for transfer. In contrast, CoSDA exhibits superior transferability, surpassing GSFDA by 4.02% on average and CoTTA



(a) Vanilla (b) CoSDA (c) w.o. Dual-Speed

Figure 5. The t-SNE visualizations of the features on VisDA extracted by Vanilla, CoSDA and CoSDA w.o. dual-speed. Red color denotes the source feature and blue color denotes the target feature. The foreground points denote the data feature, while the background lattice represent the overall feature distributions.

by 5.23%, and also outperforms GSFDA in terms of BWT.

4.4. Ablation Study: Why CoSDA Works

In this section, we perform an ablation study to investigate the mechanisms underlying CoSDA’s transferability and forgetting prevention. We approach this through both quantitative and qualitative analysis, focusing on the adaptation performance and feature visualization. As discussed in Section 3, we design a teacher-student structure as well as a consistency loss to enable adaptation and utilize dual-speed optimization to prevent forgetting. Specifically, we employ mixup to generate pseudo-labels for the consistency loss and introduce MI loss to enhance robustness to hard domains.

First, we conduct domain adaptation on VisDA to validate our claims. As shown in the lower part of Table 3, we investigate the contributions of each part in our method by successively removing the teacher model, dual-speed optimization, mixup, and MI loss. The first row of the table shows that removing the teacher model and using only the student model for predictions leads to overfitting to certain classes and complete failure of adaptation, highlighting the importance of the teacher-student structure. The second row shows that removing dual-speed optimization and simultaneously updating both teacher and student models hardly affects adaptation accuracy, but leads to severe catastrophic forgetting. This highlights the crucial role of dual-speed optimization in preventing forgetting. The next three rows of the table illustrate the results of removing mixup, MI loss, and both mixup and MI loss, and the results indicate that both mixup and MI loss contribute significantly to improving the adaptation performance. We further conduct ablation study of MI loss on DomainNet. The results in Table 1 show that the removal of MI loss leads to training failure on hard domains, highlighting its crucial role in maintaining robustness.

Moreover, we visualize the features of source and target domains under three settings: vanilla, CoSDA, and CoSDA without dual-speed optimization, as shown in Figure 5. Vanilla shows significant distribution shift between source and target domains. After adaptation with CoSDA,

we observe that the model learns a shared feature space for both source and target domains, indicating its ability to achieve transferability and prevent catastrophic forgetting. However, without the application of dual-speed optimization, we observe that while some distances between source-target features decrease, others remain distant, suggesting the occurrence of catastrophic forgetting.

5. Conclusion

In summary, this work conducts a systematic investigation into the issue of catastrophic forgetting on existing domain adaptation methods and introduces a practical DA task named continual source-free domain adaptation. CoSDA, a dual-speed optimized teacher-student consistency learning method, is proposed to mitigate forgetting and enable multi-target sequential adaptation. Extensive evaluations show that CoSDA outperforms state-of-the-art methods with better transferability-stability trade-off, making it a strong baseline for future studies. In addition, our open-source unified implementation framework designed for different SFDA methods can serve as a foundation for further explorations.

References

- [1] Sk Miraj Ahmed, Dripta S. Raychaudhuri, Sujoy Paul, Samet Oymak, and Amit K. Roy-Chowdhury. Unsupervised multi-source domain adaptation without access to source data. In *CVPR*, 2021. 5
- [2] Mohammad Al-Rubaie and J. Morris Chang. Privacy-preserving machine learning: Threats and solutions. *IEEE Secur. Priv.*, 17(2):49–58, 2019. 1
- [3] Shai Ben-David, John Blitzer, Koby Crammer, Alex Kulesza, Fernando Pereira, and Jennifer Wortman Vaughan. A theory of learning from different domains. *Machine Learning*, 79(1-2):151–175, 2010. 1
- [4] David Berthelot, Nicholas Carlini, Ian Goodfellow, Nicolas Papernot, Avital Oliver, and Colin A Raffel. Mixmatch: A holistic approach to semi-supervised learning. In *NeurIPS*, 2019. 4, 5
- [5] Andreea Bobu, Eric Tzeng, Judy Hoffman, and Trevor Darrell. Adapting to continuously shifting domains. In *ICLR Workshop*, 2018. 1, 3
- [6] Luigi Carratino, Moustapha Cissé, Rodolphe Jenatton, and Jean-Philippe Vert. On mixup regularization. *J. Mach. Learn. Res.*, 23(325):1–31, 2022. 4, 12, 13
- [7] Woong-Gi Chang, Tackgeun You, Seonguk Seo, Suha Kwak, and Bohyung Han. Domain-specific batch normalization for unsupervised domain adaptation. In *CVPR*, 2019. 4
- [8] Ting Chen, Simon Kornblith, Mohammad Norouzi, and Geoffrey Hinton. A simple framework for contrastive learning of visual representations. In *ICML*, 2020. 4
- [9] Weijie Chen, LuoJun Lin, Shicai Yang, Di Xie, Shiliang Pu, and Yueting Zhuang. Self-supervised noisy label learning for source-free unsupervised domain adaptation. In *IROS*, pages 10185–10192. IEEE, 2022. 3
- [10] Ekin Dogus Cubuk, Barret Zoph, Dandelion Mané, Vijay Vasudevan, and Quoc V. Le. Autoaugment: Learning augmentation policies from data. In *CVPR*, 2019. 4, 15
- [11] Zhijie Deng, Yucen Luo, and Jun Zhu. Cluster alignment with a teacher for unsupervised domain adaptation. In *ICCV*, 2019. 13
- [12] Haozhe Feng, Zhaoyang You, Minghao Chen, Tianye Zhang, Minfeng Zhu, Fei Wu, Chao Wu, and Wei Chen. KD3A: unsupervised multi-source decentralized domain adaptation via knowledge distillation. In *ICML*, 2021. 7
- [13] Yaroslav Ganin, Evgeniya Ustinova, Hana Ajakan, Pascal Germain, Hugo Larochelle, François Laviolette, Mario Marchand, and Victor S. Lempitsky. Domain-adversarial training of neural networks. *J. Mach. Learn. Res.*, 17:59:1–59:35, 2016. 1, 14
- [14] Jean-Bastien Grill, Florian Strub, Florent Altché, Corentin Tallec, Pierre H. Richemond, Elena Buchatskaya, Carl Doersch, Bernardo Ávila Pires, Zhaohan Guo, Mohammad Gheshlaghi Azar, Bilal Piot, Koray Kavukcuoglu, Rémi Munos, and Michal Valko. Bootstrap your own latent - A new approach to self-supervised learning. In *NeurIPS*, 2020. 5
- [15] Hongyu Guo, Yongyi Mao, and Richong Zhang. Augmenting data with mixup for sentence classification: An empirical study. *arXiv preprint*, 2019. 4

- [16] Raia Hadsell, Dushyant Rao, Andrei A Rusu, and Razvan Pascanu. Embracing change: Continual learning in deep neural networks. *Trends in cognitive sciences*, 24(12):1028–1040, 2020. 5
- [17] Kaiming He, Haoqi Fan, Yuxin Wu, Saining Xie, and Ross B. Girshick. Momentum contrast for unsupervised visual representation learning. In *CVPR*, 2020. 5
- [18] Geoffrey Hinton, Oriol Vinyals, and Jeff Dean. Distilling the knowledge in a neural network. *arXiv preprint*, 2015. 3, 5
- [19] Sepp Hochreiter and Jürgen Schmidhuber. Long short-term memory. *Neural Comput.*, 9(8):1735–1780, 1997. 3
- [20] Judy Hoffman, Eric Tzeng, Taesung Park, Jun-Yan Zhu, Phillip Isola, Kate Saenko, Alexei Efros, and Trevor Darrell. Cycada: Cycle-consistent adversarial domain adaptation. In *ICML*, 2018. 1
- [21] Weihua Hu, Takeru Miyato, Seiya Tokui, Eiichi Matsumoto, and Masashi Sugiyama. Learning discrete representations via information maximizing self-augmented training. In *ICML*, 2017. 4, 13
- [22] James Kirkpatrick, Razvan Pascanu, Neil Rabinowitz, Joel Veness, Guillaume Desjardins, Andrei A Rusu, Kieran Milan, John Quan, Tiago Ramalho, Agnieszka Grabska-Barwinska, et al. Overcoming catastrophic forgetting in neural networks. *Proceedings of the national academy of sciences*, 114(13):3521–3526, 2017. 3
- [23] Jogendra Nath Kundu, Akshay R. Kulkarni, Suvaansh Bhambri, Deepesh Mehta, Shreyas Anand Kulkarni, Varun Jampani, and Venkatesh Babu Radhakrishnan. Balancing discriminability and transferability for source-free domain adaptation. In *ICML*, 2022. 2, 3, 5
- [24] Jogendra Nath Kundu, Naveen Venkat, Ambareesh Revanur, R Venkatesh Babu, et al. Towards inheritable models for open-set domain adaptation. In *CVPR*, 2020. 1
- [25] Timothée Lesort, Vincenzo Lomonaco, Andrei Stoian, Davide Maltoni, David Filliat, and Natalia Díaz Rodríguez. Continual learning for robotics: Definition, framework, learning strategies, opportunities and challenges. *Inf. Fusion*, 58:52–68, 2020. 1
- [26] Rui Li, Qianfen Jiao, Wenming Cao, Hau-San Wong, and Si Wu. Model adaptation: Unsupervised domain adaptation without source data. In *CVPR*, 2020. 1, 3
- [27] Wei Li, Kefeng Fan, and Huihua Yang. Teacher–student mutual learning for efficient source-free unsupervised domain adaptation. *Knowledge-Based Systems*, 261:110204, 2023. 3
- [28] Xiaoxiao Li, Meirui Jiang, Xiaofei Zhang, Michael Kamp, and Qi Dou. Fed{bn}: Federated learning on non-{iid} features via local batch normalization. In *ICLR*, 2021. 4
- [29] Jian Liang, Dapeng Hu, and Jiashi Feng. Do we really need to access the source data? source hypothesis transfer for unsupervised domain adaptation. In *ICML*, 2020. 1, 2, 3, 4, 5, 13, 14
- [30] Jian Liang, Dapeng Hu, Jiashi Feng, and Ran He. Dine: Domain adaptation from single and multiple black-box predictors. In *CVPR*, 2022. 3, 5
- [31] Jian Liang, Dapeng Hu, Yunbo Wang, Ran He, and Jiashi Feng. Source data-absent unsupervised domain adaptation through hypothesis transfer and labeling transfer. *IEEE Trans. Pattern Anal. Mach. Intell.*, 44(11):8602–8617, 2022. 1, 2, 3, 5
- [32] Mingsheng Long, Yue Cao, Jianmin Wang, and Michael I. Jordan. Learning transferable features with deep adaptation networks. In *ICML*, 2015. 1, 14
- [33] David Lopez-Paz and Marc’Aurelio Ranzato. Gradient episodic memory for continual learning. *NeurIPS*, 30, 2017. 5
- [34] Alexander Lyzhov, Yuliya Molchanova, Arsenii Ashukha, Dmitry Molchanov, and Dmitry P. Vetrov. Greedy policy search: A simple baseline for learnable test-time augmentation. In *UAI*, 2020. 4
- [35] Arun Mallya and Svetlana Lazebnik. Packnet: Adding multiple tasks to a single network by iterative pruning. In *CVPR*, pages 7765–7773, 2018. 3
- [36] Massimiliano Mancini, Samuel Rota Buló, Barbara Caputo, and Elisa Ricci. Adagraph: Unifying predictive and continuous domain adaptation through graphs. In *CVPR*, pages 6568–6577, 2019. 3
- [37] Linghui Meng, Jin Xu, Xu Tan, Jindong Wang, Tao Qin, and Bo Xu. Mixspeech: Data augmentation for low-resource automatic speech recognition. In *ICASSP*, 2021. 4
- [38] Payman Mohassel and Yupeng Zhang. Secureml: A system for scalable privacy-preserving machine learning. In *IEEE Symposium on Security and Privacy*, 2017. 1
- [39] Shuaicheng Niu, Jiaxiang Wu, Yifan Zhang, Yafo Chen, Shijian Zheng, Peilin Zhao, and Mingkui Tan. Efficient test-time model adaptation without forgetting. In *ICML*, pages 16888–16905, 2022. 3
- [40] Xingchao Peng, Qinxun Bai, Xide Xia, Zijun Huang, Kate Saenko, and Bo Wang. Moment matching for multi-source domain adaptation. In *ICCV*, 2019. 2, 5, 7
- [41] Xingchao Peng, Ben Usman, Neela Kaushik, Judy Hoffman, Dequan Wang, and Kate Saenko. Visda: The visual domain adaptation challenge. *CoRR*, 2017. 2, 5
- [42] Zhen Qiu, Yifan Zhang, Hongbin Lin, Shuaicheng Niu, Yanxia Liu, Qing Du, and Mingkui Tan. Source-free domain adaptation via avatar prototype generation and adaptation. In *IJCAI*, 2021. 5
- [43] Kate Saenko, Brian Kulis, Mario Fritz, and Trevor Darrell. Adapting visual category models to new domains. In Kostas Daniilidis, Petros Maragos, and Nikos Paragios, editors, *ECCV*, 2010. 2, 5
- [44] Kuniaki Saito, Kohei Watanabe, Yoshitaka Ushiku, and Tatsuya Harada. Maximum classifier discrepancy for unsupervised domain adaptation. In *CVPR*, 2018. 1
- [45] Khadija Shaheen, Muhammad Abdullah Hanif, Osman Hasan, and Muhammad Shafique. Continual learning for real-world autonomous systems: Algorithms, challenges and frameworks. *J. Intell. Robot. Syst.*, 105(1):9, 2022. 1
- [46] Xavier Soria, Edgar Riba, and Ángel D. Sappa. Dense extreme inception network: Towards a robust CNN model for edge detection. In *WACV*, pages 1912–1921, 2020. 7, 15
- [47] Shixiang Tang, Peng Su, Dapeng Chen, and Wanli Ouyang. Gradient regularized contrastive learning for continual domain adaptation. In *AAAI*, 2021. 1

- [48] Antti Tarvainen and Harri Valpola. Mean teachers are better role models: Weight-averaged consistency targets improve semi-supervised deep learning results. In *NeurIPS*, pages 1195–1204, 2017. 3
- [49] Hemanth Venkateswara, Jose Eusebio, Shayok Chakraborty, and Sethuraman Panchanathan. Deep hashing network for unsupervised domain adaptation. In *CVPR*, 2017. 2, 5
- [50] Qin Wang, Olga Fink, Luc Van Gool, and Dengxin Dai. Continual test-time domain adaptation. In *CVPR*, 2022. 1, 2, 3, 4, 5
- [51] Shiqi Yang, Yaxing Wang, Joost Van De Weijer, Luis Herranz, and Shangling Jui. Unsupervised domain adaptation without source data by casting a bait. *arXiv preprint*, 2020. 5
- [52] Shiqi Yang, Yaxing Wang, Joost van de Weijer, Luis Herranz, and Shangling Jui. Exploiting the intrinsic neighborhood structure for source-free domain adaptation. In *NeurIPS*, 2021. 2, 3, 5, 14
- [53] Shiqi Yang, Yaxing Wang, Joost van de Weijer, Luis Herranz, and Shangling Jui. Generalized source-free domain adaptation. In *ICCV*, 2021. 1, 2, 3, 5
- [54] Shiqi Yang, Yaxing Wang, Kai Wang, Shangling Jui, and Joost van de Weijer. Attracting and dispersing: A simple approach for source-free domain adaptation. In *NeurIPS*, 2022. 2, 3, 5
- [55] Hongyi Zhang, Moustapha Cissé, Yann N. Dauphin, and David Lopez-Paz. mixup: Beyond empirical risk minimization. In *ICLR*, 2018. 4
- [56] Linjun Zhang, Zhun Deng, Kenji Kawaguchi, Amirata Ghorbani, and James Zou. How does mixup help with robustness and generalization? In *ICLR*, 2021. 4
- [57] Yuchen Zhang, Tianle Liu, Mingsheng Long, and Michael I. Jordan. Bridging theory and algorithm for domain adaptation. In *ICML*, 2019. 5
- [58] Ziyi Zhang, Weikai Chen, Hui Cheng, Zhen Li, Siyuan Li, Liang Lin, and Guanbin Li. Divide and contrast: Source-free domain adaptation via adaptive contrastive learning. In *NeurIPS*, 2022. 2, 3, 5, 14
- [59] Sicheng Zhao, Guangzhi Wang, Shanghang Zhang, Yang Gu, Yaxian Li, Zhichao Song, Pengfei Xu, Runbo Hu, Hua Chai, and Kurt Keutzer. Multi-source distilling domain adaptation. In *AAAI*, 2020. 3

A. Further Analyses

A.1. The Rationale of Selecting Mixup as Data Augmentation Strategy

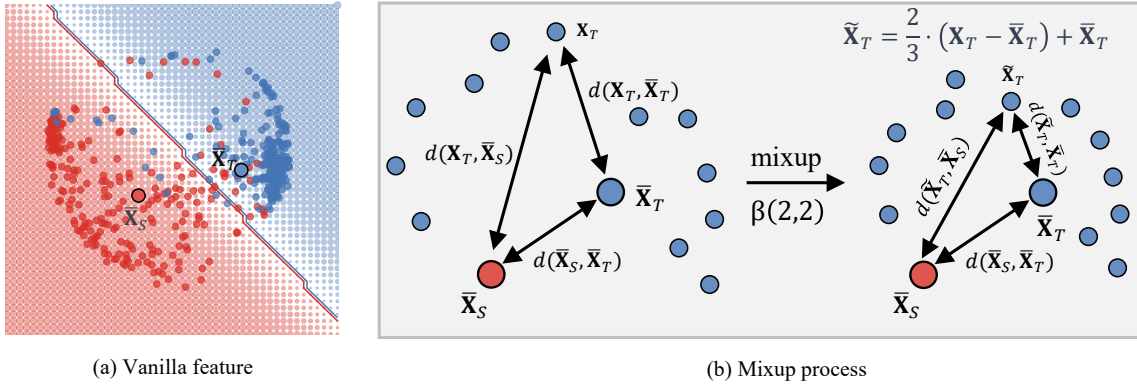


Figure 6. An overview of mixup process on VisDA. **Red color** denotes the source feature and **blue color** denotes the target feature. The centroids of source and target features are denoted by $\bar{\mathbf{X}}_S$ and $\bar{\mathbf{X}}_T$. For CoSDA, we set the value of $\beta(a, a)$ to $a = 2$ and use $\bar{\lambda} = \frac{2}{3}$. The mixup process results in data points shrinking to their centroids, thereby reducing the distance between the source and target domains.

In Section 3.1, we introduce mixup as a data augmentation strategy used in CoSDA, which is claimed to holistically reduce the domain distance and thereby facilitating the learning of domain-invariant features. In this section, We provide evidence to support this claim. We start with summarizing an equivalent form of mixup proposed by [6] which establishes a connection with label-smoothing techniques as follows:

Theorem A.1. *Let \mathbb{D}_T be the target domain with N training samples \mathbf{X}_i and their corresponding pseudo-labels \mathbf{p}_i . Suppose the mixup augmentation with distribution $\beta_{[0,1]}(a, a)$ are used for the student model h_{ψ} with the consistency loss $\ell_{\text{cons}}(\cdot)$. Then, the empirical risk of the consistency loss can be approximated as:*

$$\xi_{\text{mixup}}(\ell_{\text{cons}}, h_{\psi}) := \frac{1}{N} \sum_{i=1}^N \mathbb{E}_{j, \theta} \left[\ell_{\text{cons}}(\tilde{\mathbf{X}}_i + \delta_i, \tilde{\mathbf{p}}_i + \epsilon_i; \psi) \right], \quad (5)$$

where $j \sim \text{Unif}(1, \dots, N)$, $\theta \sim \beta_{[\frac{1}{2}, 1]}(a, a)$, and $(\tilde{\mathbf{X}}_i, \tilde{\mathbf{p}}_i, \delta_i, \epsilon_i)$ can be formulated by squeezing the samples towards their centroid $\bar{\mathbf{X}} = \frac{1}{N} \sum_{i=1}^N \mathbf{X}_i$ as follows:

$$\begin{cases} \tilde{\mathbf{X}}_i = \bar{\theta}(\mathbf{X}_i - \bar{\mathbf{X}}) + \bar{\mathbf{X}}, \\ \tilde{\mathbf{p}}_i = \bar{\theta}(\mathbf{p}_i - \bar{\mathbf{p}}) + \bar{\mathbf{p}}, \\ \delta_i = (\theta - \bar{\theta})\mathbf{X}_i + (1 - \theta)\mathbf{X}_j - (1 - \bar{\theta})\bar{\mathbf{X}}, \\ \epsilon_i = (\theta - \bar{\theta})\mathbf{p}_i + (1 - \theta)\mathbf{p}_j - (1 - \bar{\theta})\bar{\mathbf{p}}, \end{cases} \quad (6)$$

where δ_i, ϵ_i are zero-mean random perturbations, $\|\delta_i\|_2 \ll \|\mathbf{X}_i\|_2$ and $\bar{\theta} = 2 - \frac{a(a-1)}{a-\frac{1}{2}}$ is the expectation of distribution $\theta \sim \beta_{[1/2, 1]}(a, a)$. For CoSDA, we have $\bar{\theta} = \frac{2}{3}$ with $a = 2$.

Proof. We recap the format of ξ_{mixup} as follows:

$$\xi_{\text{mixup}}(\ell_{\text{cons}}, h_{\psi}) := \frac{1}{N^2} \sum_{i=1}^N \sum_{j=1}^N \mathbb{E}_{\lambda} [\ell_{\text{cons}}(h_{\psi}(\lambda\mathbf{X}_i + (1 - \lambda)\mathbf{X}_j, \lambda\mathbf{p}_i + (1 - \lambda)\mathbf{p}_j))], \quad (7)$$

where $\lambda \sim \beta_{[0,1]}(a, a)$. To investigate the impact of λ on Eq. (7), we construct a function that relates the value of λ to mixup data pairs as $m_{i,j}(\lambda)$:

$$m_{i,j}(\lambda) = \ell_{\text{cons}}(h_{\psi}(\lambda\mathbf{X}_i + (1 - \lambda)\mathbf{X}_j, \lambda\mathbf{p}_i + (1 - \lambda)\mathbf{p}_j)). \quad (8)$$

Denoting $\lambda = (1 - \pi)\theta + \pi\theta'$, $\theta \sim \beta_{[\frac{1}{2}, 1]}(a, a)$, $\theta' \sim \beta_{[0, \frac{1}{2}]}(a, a)$, $\pi \sim \text{Ber}(\frac{1}{2})$, we can rewrite $m_{i,j}(\lambda)$ as

$$\mathbb{E}_\lambda [m_{i,j}(\lambda)] = \mathbb{E}_{\theta, \theta', \pi} [m_{i,j}((1 - \pi)\theta + \pi\theta')] = \frac{1}{2} (\mathbb{E}_\theta [m_{i,j}(\theta)] + \mathbb{E}_{\theta'} [m_{i,j}(\theta')]). \quad (9)$$

Since $\theta' = 1 - \theta$, we have $\mathbb{E}_\theta [m_{i,j}(\theta)] = \mathbb{E}_{\theta'} [m_{i,j}(\theta')]$. Substituting it into Eq. (7), we obtain:

$$\xi_{\text{mixup}}(\ell_{\text{cons}}, h_\psi) = \frac{1}{N^2} \sum_{i=1}^N \sum_{j=1}^N \mathbb{E}_\theta [m_{i,j}(\theta)] = \frac{1}{N} \sum_{i=1}^N \left(\frac{1}{N} \sum_{j=1}^N \mathbb{E}_\theta [m_{i,j}(\theta)] \right). \quad (10)$$

Denote $\xi_i = \frac{1}{N} \sum_{j=1}^N \mathbb{E}_\theta [m_{i,j}(\theta)]$, we have $\xi_i = \mathbb{E}_{\theta, j} [\ell_{\text{cons}}(h_\psi(\theta \mathbf{X}_i + (1 - \theta)\mathbf{X}_j), \theta \mathbf{p}_i + (1 - \theta)\mathbf{p}_j)]$. Notably, $(\tilde{\mathbf{X}}_i, \tilde{\mathbf{p}}_i)$ has the following relation with ξ_i :

$$\tilde{\mathbf{X}}_i = \bar{\theta}(\mathbf{X}_i - \bar{\mathbf{X}}) + \bar{\mathbf{X}} = \mathbb{E}_{\theta, j} [\theta \mathbf{X}_i + (1 - \theta)\mathbf{X}_j]; \quad \tilde{\mathbf{p}}_i = \bar{\theta}(\mathbf{p}_i - \bar{\mathbf{p}}) + \bar{\mathbf{p}} = \mathbb{E}_{\theta, j} [\theta \mathbf{p}_i + (1 - \theta)\mathbf{p}_j]. \quad (11)$$

With the relations in Eq. (11), we denote ϵ , δ and prove Eq. (5) as follows

$$\delta_i = \theta \mathbf{X}_i + (1 - \theta)\mathbf{X}_j - \tilde{\mathbf{X}}_i; \quad \epsilon_i = \theta \mathbf{p}_i + (1 - \theta)\mathbf{p}_j - \tilde{\mathbf{p}}_i; \quad \xi_i = \mathbb{E}_{\theta, j} \left[\ell_{\text{cons}} \left(h_\psi(\tilde{\mathbf{X}}_i + \delta_i), \tilde{\mathbf{p}}_i + \epsilon_i \right) \right], \quad (12)$$

Combining the equations Eq. (11) and Eq. (12), we can obtain $\mathbb{E}[\delta_i] = 0$ and $\mathbb{E}[\epsilon_i] = 0$. Furthermore, following the empirical study in [6], we can conclude that the ℓ_2 -norm of δ_i is much smaller than that of \mathbf{X}_i . \square

We conduct the following analysis of Theorem A.1. Since the magnitude of the perturbation $\|\delta\|_2$ is much smaller than the norm of the mixed samples $\|\tilde{\mathbf{X}}\|_2$ [6], we can interpret the mixup augmentation as squeezing the samples towards their centroid, i.e., $\mathbf{X} \rightarrow \tilde{\mathbf{X}}$. In domain adaptation, the cluster distance between source and target domains [11] is often used to measure the degree of distribution shift. As shown in Figure 6, a source-domain-trained model has a clear boundary in the distributions of source and target domains (as shown in (a)). However, the centroids of the source and target domains are much closer than the sample points. By using the mixup method, all sample points are squeezed towards the centroids (as shown in (b)), thereby heuristically reducing the domain distance and facilitating the learning of domain-invariant features.

A.2. The Analysis of Mutual Information Loss

Mutual information (MI) is a concept used to quantify the degree of dependence between two random variables. It measures the reduction in uncertainty of one variable by knowing the value of the other variable, indicating the amount of information they share. The mutual information between two random variables \mathbf{X} and \mathbf{y} is defined as follows:

$$\text{MI}(\mathbf{X}, \mathbf{y}) = D_{\text{KL}}(p(\mathbf{X}, \mathbf{y}) \| p(\mathbf{X})p(\mathbf{y})). \quad (13)$$

During the training process of CoSDA, we use \mathbf{y} to denote the label and use $h_\psi(\mathbf{X})$ as the label distribution $p(\mathbf{y}|\mathbf{X})$. For B samples in a mini-batch, we estimate the distribution of data \mathbf{X} using empirical distribution as $p(\mathbf{X}) = \frac{1}{B}$. Then we estimate $p(\mathbf{y})$ as $p(\mathbf{y}) = \sum_{\mathbf{X}} p(\mathbf{y}|\mathbf{X})p(\mathbf{X}) = \frac{1}{B} \sum_{i=1}^B h_\psi(\mathbf{X}_i) := \bar{\mathbf{h}}_\psi$. Based on the definitions above, the mutual information for CoSDA can be expressed as follows:

$$\text{MI}(\{\mathbf{X}_i\}_{i=1}^B, \psi) = -\frac{1}{B} D_{\text{KL}}(h_\psi(\mathbf{X}_i) \| \bar{\mathbf{h}}_\psi), \quad (14)$$

and the mutual information loss is $\ell_{\text{MI}} := -\text{MI}(\{\mathbf{X}_i\}_{i=1}^B, \psi)$.

In Section 3.2, we claim the mutual information loss can improve the robustness of the model and enable it to learn from hard domains. We provide evidence to support this claim. Based on previous studies [29, 21], ℓ_{MI} can be decomposed into two components: maximizing the instance entropy and minimizing the marginal inference entropy:

1. Maximize instance entropy:

$$\max_{\psi} \frac{1}{B} \sum_{i=1}^B \text{ent}(h_\psi(\mathbf{X}_i)) := \max_{\psi} \frac{1}{B} \sum_{i=1}^B \sum_{c=1}^C -h_\psi(\mathbf{X}_i)_{i,c} \log h_\psi(\mathbf{X}_i)_{i,c}. \quad (15)$$

Table 4. Hyperparameters for all the methods evaluated in the experiments.

Method	Shared hyperparameters	Dataset specific hyperparameters
SHOT&SHOT++	learning rate: $1 \times 10^{-3} \sim 2 \times 10^{-4}$ for backbone; learning rate: $1 \times 10^{-2} \sim 2 \times 10^{-3}$ for bottleneck and classifier; cls_loss weight: 0.3; ent_loss weight: 1.0; ssl_loss weight: 0.6 (for SHOT++).	Same for all datasets.
NRC	learning rate: $2 \times 10^{-3} \sim 1 \times 10^{-3}$; $k = 4, m = 3$.	For VisDA, set learning rate: $2 \times 10^{-3} \sim 1 \times 10^{-4}, k = 8, m = 8$; For DomainNet, set $k = 6, m = 4$.
AaD	learning rate: $2 \times 10^{-3} \sim 1 \times 10^{-3}$; $\alpha = 0.4, \text{decay } \gamma = 0.96$.	For VisDA, set learning rate: $2 \times 10^{-3} \sim 1 \times 10^{-4}$; $k = 2, 3, 4, 8$ For Office-Home, Office31, DomainNet, VisDA.
DaC	learning rate: $2 \times 10^{-3} \sim 2 \times 10^{-4}$; temperature: 0.05, K: 40, k: 5; momentum: 0.8, threshold: 0, gate: 0.97; coefficients for cls, im, con and mmd: (0.02, 0.25, 0.03, 0.15).	For VisDA, set learning rate: $5 \times 10^{-4} \sim 6 \times 10^{-5}$; K: 300, momentum: 0.2; coefficients for cls, im, con and mmd: (0.39, 0.1, 1.0, 0.3) ; For DomainNet, set learning rate: $1 \times 10^{-3} \sim 2 \times 10^{-4}$.
EdgeMix	learning rate: $1 \times 10^{-3} \sim 2 \times 10^{-4}$; $\lambda = 0.9, \text{finetune epochs: } 2$.	For Office31, learning rate: $2 \times 10^{-3} \sim 1 \times 10^{-3}$; For VisDA, learning rate: $2 \times 10^{-3} \sim 1 \times 10^{-4}$.
GSFDA	learning rate: $1 \times 10^{-3} \sim 2 \times 10^{-4}$ for backbone; learning rate: $1 \times 10^{-4} \sim 2 \times 10^{-5}$ for bottleneck and classifier; $k = 2, s = 100, \lambda_{gen} : 1$.	For VisDA, set $k = 10$; For DomainNet, set backbone learning rate: $5 \times 10^{-4} \sim 1 \times 10^{-5}$; bottleneck and classifier learning rate: $5 \times 10^{-5} \sim 1 \times 10^{-6}$; $k = 10, \lambda_{gen} = 2$.
CoTTA	source model preserve ratio (rst): 0.01; average predictive prob (ap): 0.92; aug times: 32.	For Office31 and VisDA, set ap to 0.5 and rst to 0.001.
CoSDA	learning rate: $2 \times 10^{-3} \sim 1 \times 10^{-3}$; temperature: $\tau = 0.07$; mixup: $\beta(2, 2)$; loss weight $\alpha = 1$; EMA momentum: $m = [0.9, 0.99]$.	For DomainNet, set $\alpha = 0.1$ and $m = [0.95, 0.99]$; For VisDA, set learning rate: $4 \times 10^{-3} \sim 2 \times 10^{-3}$.

2. Minimize marginal entropy:

$$\min_{\psi} \text{ent}(\bar{\mathbf{h}}_{\psi}) := \min_{\psi} \sum_{c=1}^C -\bar{\mathbf{h}}_{\psi,c} \log \bar{\mathbf{h}}_{\psi,c}. \quad (16)$$

By maximizing instance entropy, the model learns to assign distinct semantics for each data, resulting in a concentrated classification distribution. This enables the model to learn classification information even in the presence of inaccurate pseudo-labels in hard domains. By minimizing the marginal entropy, we ensure that the model learns a uniform marginal distribution, which allows it to learn information from all classes in a broad and balanced manner, rather than overfitting to a few specific classes. Based on the above two advantages, we demonstrate that integrating mutual information loss into the training objective can lead to good properties such as improved robustness and effective learning from hard domains.

B. Implementation Details and Model-specific Hyperparameters for Realistic Evaluation

B.1. Training Paradigm

In our experiments, we follow previous settings [32, 13, 29, 52, 58] and utilize two common training paradigms: inductive learning and transductive learning. For DomainNet that provides an official train-test split, we use the inductive learning pipeline to train models on the training set and report model performance on the test set. On the other hand, for OfficeHome, Office31, and VisDA, which do not provide an official train-test split, most methods adopt the transductive learning based adaptation pipeline. In this pipeline, the training and testing datasets are identical. Specifically, models are trained on the entire source domain and adapted to the entire unlabeled target domain. During testing, the models are evaluated on the same training dataset to report the adaptation performance as well as the degree of catastrophic forgetting. It is important to note that, since the inductive learning paradigm is more practical, we primarily focus on the analysis and discussion of our results based on the DomainNet experiments, supplemented by the transductive learning performance on the other three benchmarks.

B.2. Hyperparameters

We build a unified implementation for all methods with the following settings: we use ResNet50 as the backbone for DomainNet, OfficeHome, and Office31, and ResNet101 for VisDA. We apply cyclic cosine annealing as the learning rate schedule, set the weight decay to 5×10^{-3} , and use random horizontal flip as regular data augmentations, except for DaC, EdgeMix, and CoTTA. Specifically, EdgeMix uses a pretrained DexiNed [46] to extract and confuse edge features, while DaC and CoTTA use AutoAug [10] as augmentation strategies.

In addition, we construct a validation dataset to select suitable model-specific hyperparameters. Specifically, we split 5% of the data from the current target domain’s training set as the validation dataset. In the CoSDA setting, we are not allowed to access the data from previous domains. Therefore, we do not construct a validation dataset on the source domain or previously encountered target domains. The details of hyperparameter selection for each method are presented in Table 4.